OL | Organic Letters

Letter

Cite This: Org. Lett. XXXX, XXX, XXX−XXX

pubs.acs.org/OrgLett

Network Analysis of Substituted Bullvalenes

Oussama Yahiaoui,[†,‡] Lukáš F. Pašteka,[*,§] Christopher J. Blake,[∥] Christopher G. Newton,[†] and Thomas Fallon[*,†,‡]

[†]Department of Chemistry, The University of Adelaide, Adelaide, SA 5005, Australia

[‡]Institute of Natural and Mathematical Sciences, Massey University, Auckland 0632, New Zealand

[§]Department of Physical and Theoretical Chemistry, Faculty of Natural Sciences, Comenius University, Bratislava, Slovakia

[∥]Research School of Chemistry, Australian National University, Canberra, ACT 0200, Australia

Supporting Information

ABSTRACT: Substituted bullvalenes are dynamic shape-shifting molecules that exist within complex reaction networks. Herein, we report the synthesis of di- and trisubstituted bullvalenes and investigate their dynamic properties. Trisubstituted bullvalenes share a common major isomer which shows kinetic metastability. A survey of the thermodynamic and kinetic landscapes through computational analysis together with kinetic simulation provides a map of the internal dynamics of these systems.

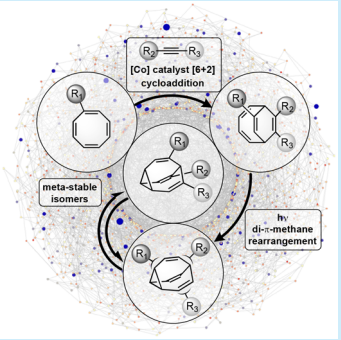

More than half a century since its prediction and initial preparation,[1,2] bullvalene (**1**) remains a source of continued intrigue. This archetypal fluxional molecule exists as an ensemble of 1 209 600 degenerate isomers through rapid Cope rearrangements (Scheme 1a). This property of *total degeneracy* is unique among stable organic structures.[3] Substituted bullvalenes are particularly interesting, as degeneracy is lost and substituents will spontaneously explore all possible structural arrangements.

Scheme 1. (a) Total Degeneracy of Bullvalene and (b) Our Synthetic Route to Trisubstituted Bullvalenes

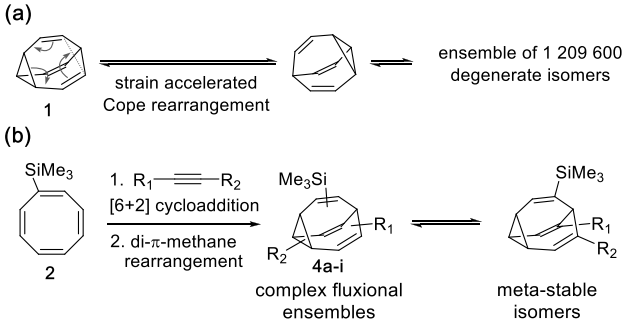

Within the rapidly advancing context of dynamic covalent chemistry,[4] the unimolecular shape-shifting nature of bullvalene suggests a range of potential applications in medicinal chemistry and molecular devices. In a series of reports, the Bode group has explored these concepts,[5] most notably in the construction of a fluxional polyol sensing array.[5e] However, the rational design of applications built on fluxional molecules remains underdeveloped.

Heavily substituted bullvalenes represent enormous reaction networks with hundreds or even thousands of unique isomers. However, the overall structure and dynamics of such systems will ultimately be governed by a small subset of low-energy isomers and isomerization pathways. A more detailed understanding of the internal dynamics of bullvalene networks will help to advance these systems toward viable applications.

The activation energy of bullvalene isomerization was first determined by Saunders at 49.4 ± 0.4 kJ/mol using VT-NMR measurements.[6] Substituted bullvalenes present increasingly complex kinetic landscapes. The only detailed kinetic study of a substituted bullvalene was by Luz who experimentally determined the kinetic parameters of all reactions within the network of fluorobullvalene.[7]

A picture of the internal energy landscapes of substituted bullvalenes has generally come from measuring the distributions of populated isomers using low-temperature NMR studies and assuming rapid equilibration at room temperature. Occasionally metastable isomers have been observed and even isolated by recrystallization[8] or chromatography.[5c] Foremost of these is a tetrasubstituted bullvalene encountered by Bode. The stability of this structure was rationalized through a computational analysis of the local network environment.[5f]

The synthesis of substituted bullvalenes has seen renewed interest with important contributions from the Bode[5] and

Received: October 22, 2019

DOI: 10.1021/acs.orglett.9b03737
Org. Lett. XXXX, XXX, XXX−XXX

Echavarren[9] groups. We recently reported an efficient two-step synthetic protocol for the synthesis of mono- and disubstituted bullvalenes.[10] The method employs cobalt-catalyzed [6 + 2] cycloaddition reactions of cyclooctatetraene[11] followed by photochemical di-π-methane rearrangement.[12] Alongside our synthetic work, we developed a computational toolbox to automate the network analysis of substituted bullvalenes and generate input structures for quantum chemical calculations for all objects in any given network. This provides a global picture of bullvalene energy landscapes.

In this paper, we extend our synthetic protocol to the preparation of trisubstituted bullvalenes through the use of a substituted cyclooctatetraene (Scheme 1b). This includes the first synthesis of heterogeneously trisubstituted bullvalenes, objects of considerable dynamic complexity, that surprisingly all share a common metastable isomer. Computational analysis coupled with kinetic simulations help rationalize this general kinetic feature.

The synthesis employs a cobalt-catalyzed [6 + 2] cycloaddition of trimethylsilylcyclooctatetraene **2**[13] and a range of substituted alkynes (Scheme 2). The bicyclo[4.2.2]deca-2,4,7,9-tetraene (BDT) intermediates **3a−g** were isolated as inconsequential mixtures of constitutional isomers.[14] A simple TBS protection of **3f** gave **3g**, which structurally differentiates the three substituents. Photochemical di-π-methane rearrangement of the BDT intermediates proceeded smoothly to give the corresponding bullvalenes in moderate yields. The alcohol **4g** and diol **4f** were oxidized under Swern conditions to give the corresponding aldehydes.

With this collection of bullvalenes in hand, we began to study their dynamic behavior. Population distributions of the ensembles were determined using low-temperature NMR experiments. Disubstituted bullvalenes **4a−e** exist within relatively simple networks.[15] In all cases the major isomer is observed, whereby both substituents flank the bridgehead position (**4a-e:A**), together with a minor isomer **4a-e:B** (Figure 1a). Room-temperature NMR analysis of trisubstituted bullvalenes **4f−i** revealed a major isomer that is not in rapid exchange with the ensemble, isomer **4f-i:A**, together with broad signals characteristic of dynamic bullvalene ensembles (Figure 1b). Low-temperature NMR measurements revealed a minor isomer **4f-i:B**, along with several others. In all cases, ^{1}H

Scheme 2. Synthesis of Substituted Bullvalenes[a]

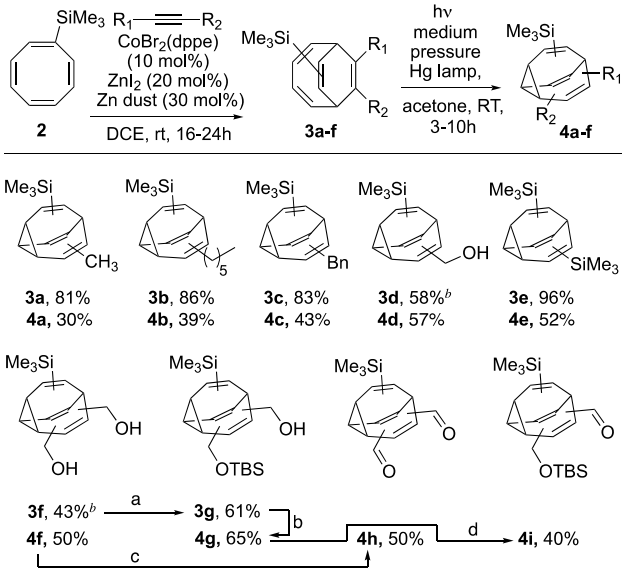

[a]Reagents and conditions: (a) NaH (3 equiv), TBSC1 (1 equiv), THF, 0 °C, 16 h. (b) Photochemical reaction conditions as above. (c) $(COCl)_2$ (2.4 equiv), DMSO (5 equiv), Et_3N (10 equiv), CH_2Cl_2 −78 °C, 1 h. (d) $(COCl)_2$ (1.3 equiv), DMSO (2.6 equiv), Et_3N (5 equiv), CH_2Cl_2 −78 °C, 1 h. [b]Reaction run with 2,2,2-trifluoroethanol as solvent at 55 °C.

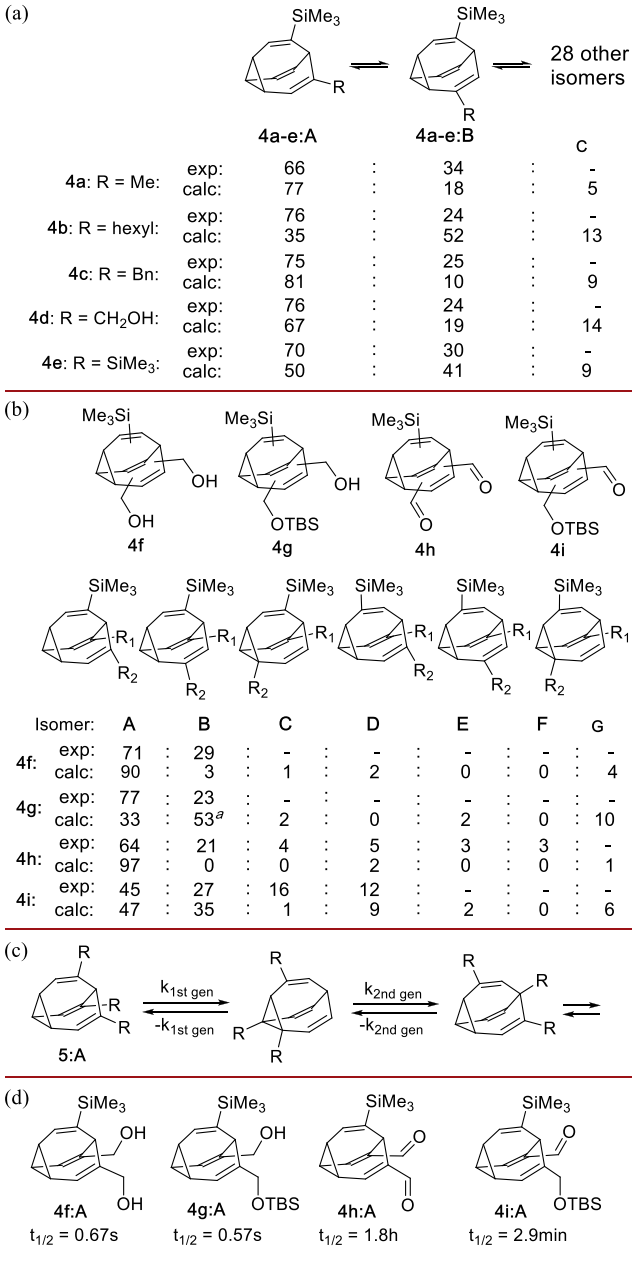

Figure 1. (a) Disubstituted isomer distributions. (b) Trisubstituted isomer distributions. Experimental and computational analysis of isomer distributions. (c) Meta-stability of trisubstituted bullvalenes. (d) Predicted half-lives of trisubstituted bullvalenes. VT-NMR experiments conducted-60 °C. Indicative experimental isomer ratios are reported as a fraction of the sum of those identified. Single-point DFT calculations at B3LYP-D3BJ/Def2-TZVPPD/CPCM solvent (chloroform) performed in Orca.[18] [a]Predicted population reported as the sum of R_1/R_2 and R_2/R_1 isomers.

DOI: 10.1021/acs.orglett.9b03737
Org. Lett. XXXX, XXX, XXX−XXX

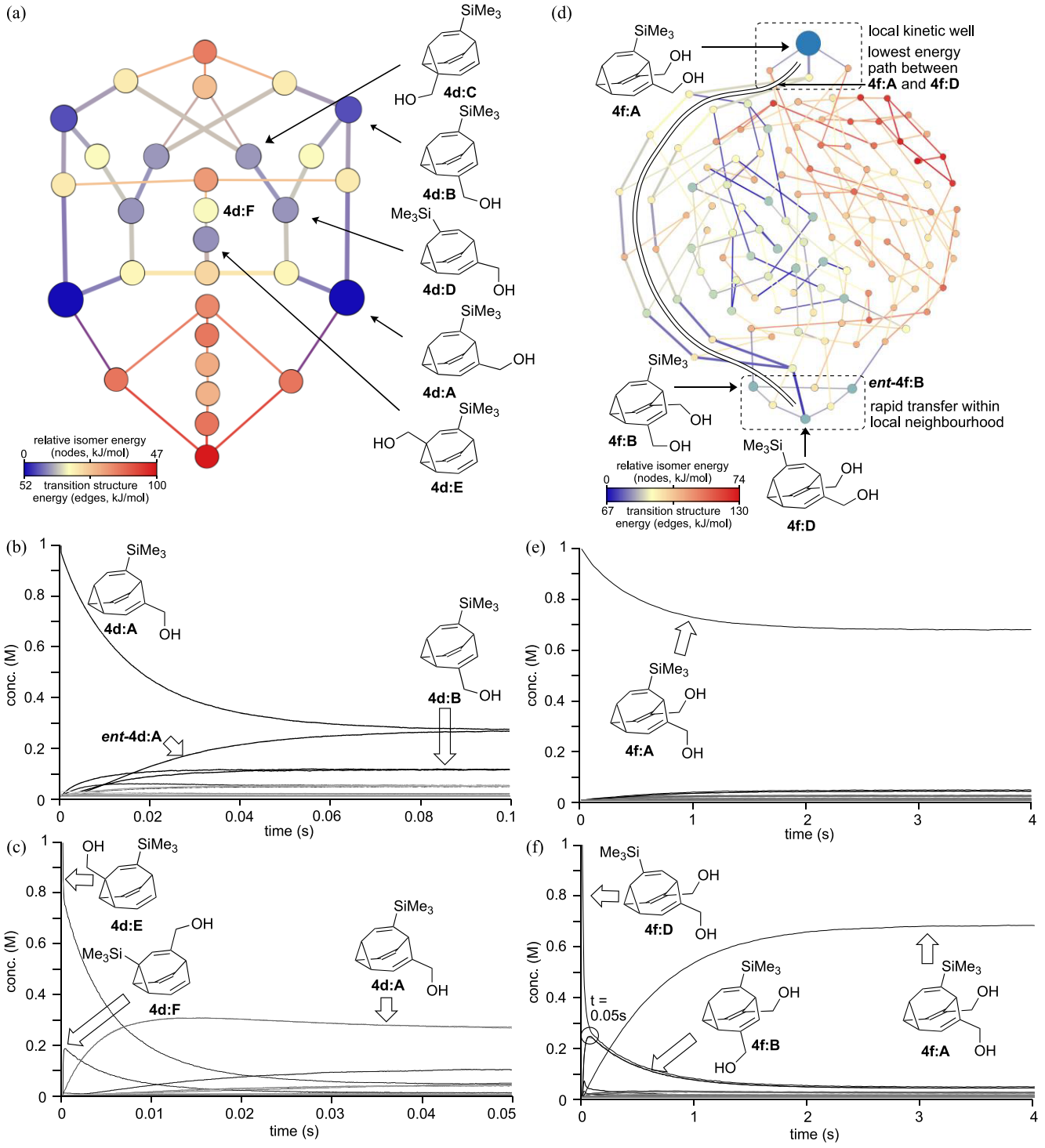

Figure 2. (a) Network graph of **4d**. (b) Simulation starting from **4d:A**. (c) Simulation starting from **4d:E**. (d) Network graph of **4f**. (e) Simulation starting from **4f:A**. (f) Simulation starting from **4f:D**.

and ^{13}C NMR spectra indicated a range of other minor isomers which could not be structurally elucidated.

Density functional theory calculations were run for all ground states and transition structures for all the ensembles studied (see SI for full details). The predicted population distributions are presented in Figure 1a,b. In all cases, the calculated population distributions are in fair agreement with experiment.

The metastability of bullvalene isomers **4f-i:A** can be rationalized by considering the local network environment of a general trisubstituted bullvalene **5:A** (Figure 1c). In order to communicate with the rest of the network, any isomer of this type must pass through two generations of relatively high-energy isomers accompanied by high-energy barriers. This combines to form a local kinetic well. Conjugating and/or sterically demanding substituents will tend to provide increased kinetic stability. This appears to be a general feature across heavily substituted bullvalenes.[16]

The local kinetic wells around bullvalenes **4f-i:A** were assessed by estimating the first- and second-generation rate

DOI: 10.1021/acs.orglett.9b03737
Org. Lett. XXXX, XXX, XXX−XXX

constants using the Eyring equation and modeling the kinetics using the *KinTek Explorer* software package.[17] This predicts room-temperature half-lives ranging from 0.57 s to 1.8 h (Figure 1d).

Reaction network diagrams provide a powerful visual tool to explore the connectivity and thermodynamic/kinetic landscapes of substituted bullvalenes. The network graphs of disubstituted bullvalene **4d** and trisubstituted bullvalene **4f** are shown in Figure 2. Nodes represent individual isomers and the edges transition structures, each color coded according to relative energy. Bullvalene **4d** exists as an ensemble of 30 isomers connected by 46 transition states. The predicted populated isomers **4d:A**−**E** are shown (though only **4d:A** and **4d:B** have been identified experimentally). This visualization reveals that the populated isomers reside within a local group connected by a set of relatively low-energy isomerization pathways. The "southern" region of the network will essentially remain unpopulated.

A complete kinetic model of **4d** was constructed by estimating all 92 first-order rate constants. Stochastic Monte Carlo simulations were run using the *Kinetiscope* software package.[19] Figure 2b shows a simulation from an initial population of the major isomer **4d:A**. The system rapidly equilibrates within 0.1 s. Initiating the simulation from the minor isomer **4d:E** illustrates the path-dependent passage of material through the system (Figure 2c).

The reaction graph of trisubstituted bullvalene **4f** is presented in Figure 2d showing all 120 isomers and 184 transition states. The major isomer **4f:A** is relatively isolated from the other populated isomers and resides within its shallow local kinetic well. Several populated isomers (calculated), **4f:B**, *ent*-**4f:B**, and **4f:D**, all reside within a local group, mutually accessible via two-step isomerizations. The lowest-energy pathway between these two regions of the network is highlighted.

A kinetic simulation from an initial population of isomer **4f:A** shows that the system reaches equilibrium within ∼1.5 s (Figure 2e). A simulation from an initial population of the minor populated isomer **4f:D** is shown in Figure 2f. In this scenario the system rapidly equilibrates toward a ∼1:1:1 mixture of **4f:D**:**4f:B**:*ent*-**4f:B** within a period of ∼0.05 s. From here the ensemble slowly generates the major isomer **4f:A** over a period of ∼2 s.

More heavily substituted bullvalenes represent a major jump in complexity, as well as a considerable synthetic challenge. However, the thermodynamic and kinetic properties of these large systems may be anticipated. To demonstrate, we ran a computational analysis of the (hypothetical) tetrasubstituted bullvalene **6** (Figure 3). With this substitution pattern there are 1640 unique isomers (852 discounting enantiomers) and 2520 transition structures. A full DFT analysis of the ground-state energies predicts only 16 isomers to be populated at room temperature with a relative abundance of greater than 1% (**6:A-P**, Figure 3). All these isomers (excepting **6:N**) have 2−3 substituents adjacent to the bridgehead, analogous to the dominant isomers of **4a**−**i**. Intriguingly, the global minimum isomer **6:A** does not have an arrangement analogous to that of **4f-i:A** and benefits from a specific intramolecular hydrogen bond, as do isomers **6:D** and **6:L**.

The full computation analysis of all transition structures represents an arduous and impractical exercise. However, surveying the likely local kinetic wells would provide useful insights. There are 28 possible isomers of **6** that maintain three

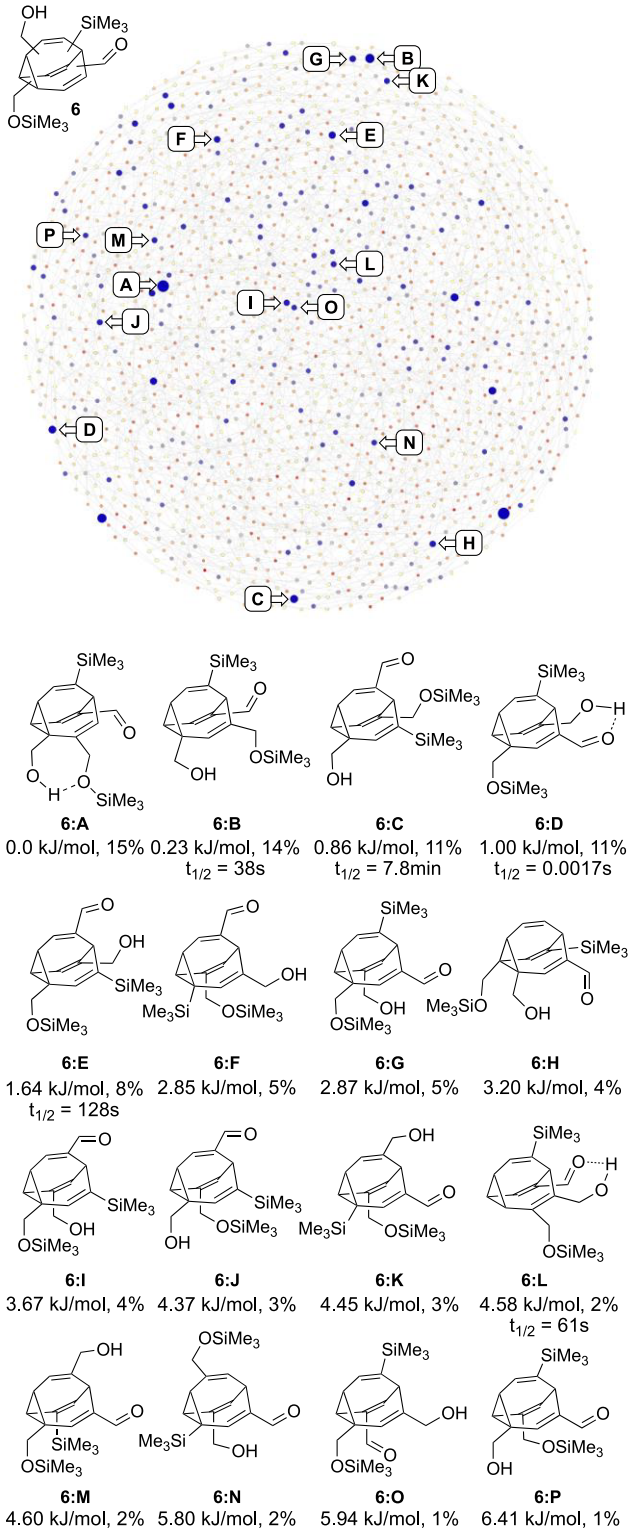

Figure 3. Network analysis of (hypothetical) tetrasubstituted bullvalene **6**. The relative stability of the predicted populated isomers **6:A-P** is shown based on single-point DFT calculations at the B3LYP-D3BJ/Def2-TZVPPD/CPCM solvent (chloroform). The predicted half-lives for isomers **6:B-E,L** is shown based on the local first- and second-generation transition structures calculated at B3LYP-D3BJ/Def2-TZVPPD(chloroform).

substituents adjacent to the bridgehead. Of these, only five reside within the pool of 16 populated isomers shown in Figure 3, **6:B-E,L**. For each of these, the first- and second-generation

DOI: 10.1021/acs.orglett.9b03737
Org. Lett. XXXX, XXX, XXX−XXX

transition structure energies were calculated, and the local kinetics modeled. The predicted half-lives range between 0.0017 s and 7.8 min. Isomer **6:D** has a surprisingly short half-life which is traced to an intramolecular hydrogen bond, stabilizing one of the first-generation transition structures (see SI for full details).

In summary, we demonstrated the synthesis of a range of disubstituted bullvalenes and the first synthesis of differentially trisubstituted bullvalenes. Low-temperature NMR experiments reveal the populated isomer distributions, in broad agreement with DFT calculations. Kinetic simulations provide a new window into the rich dynamic nature of these systems and help rationalize the meta-stability of trisubstituted bullvalene major isomers. The anticipation of kinetic and thermodynamic features within heavily substituted bullvalenes provides a framework through which to navigate these complex systems and design future shape-selective molecular devices.

■ ASSOCIATED CONTENT

Supporting Information

The Supporting Information is available free of charge on the ACS Publications website at DOI: 10.1021/acs.orglett.9b03737.

Experimental details and characterization data for all new compounds. Details of computational methods and analysis (PDF)

List of computational results (PDF)

■ AUTHOR INFORMATION

Corresponding Authors

*E-mail: thomas.fallon@adelaide.edu.au.

*E-mail: lukas.f.pasteka@gmail.com.

ORCID

Lukáš F. Pašteka: 0000-0002-0617-0524

Christopher G. Newton: 0000-0002-8962-5917

Thomas Fallon: 0000-0002-6495-5282

Notes

The authors declare no competing financial interest.

■ ACKNOWLEDGMENTS

We gratefully acknowledge the New Zealand Royal Society (Marsden Fund No. 15-MAU-154). We gratefully thank Ms. Eliza Tarcoveanu (Australian National University, Canberra) for assistance with NMR measurements. Calculations were performed using the supercomputing infrastructure of the Computing Center of the Slovak Academy of Sciences acquired in projects ITMS 26230120002 and 26210120002 supported by the Research & Development Operational Programme funded by the ERDF. LFP is grateful for the support from the Slovak Research and Development Agency (grant no. APVV-15-0105) and the Scientific Grant Agency of the Slovak Republic (grant no. 1/0777/19).

■ REFERENCES

(1) von E. Doering, W.; Roth, W. R. *Tetrahedron* **1963**, *19*, 715–737.

(2) (a) Schröder, G. *Angew. Chem., Int. Ed. Engl.* **1963**, *2*, 481–482. (b) Schröder, G. *Angew. Chem.* **1963**, *75*, 722–722.

(3) The barbaryl cation and radical represent the other totally degenerate cage hydrocarbons: (a) Ahlberg, P.; Harris, D. L.; Winstein, S. *J. Am. Chem. Soc.* **1970**, *92*, 2146–2147. (b) Ahlberg, P.; Grutzner, J. B.; Harris, D. L.; Winstein, S. *J. Am. Chem. Soc.* **1970**, *92*, 3478–3480. (c) Ahlberg, P.; Harris, D. L.; Winstein, S. *J. Am. Chem. Soc.* **1970**, *92*, 4454–4456. (d) Engdahl, C.; Ahlberg, P. J. *J. Phys. Org. Chem.* **1990**, *3*, 349–357.

(4) For recent reviews, see: (a) Rowan, S. J.; Cantrill, S. J.; Cousins, G. R. L.; Sanders, J. K. M.; Stoddart, J. F. *Angew. Chem., Int. Ed.* **2002**, *41*, 898–952. (b) Corbett, P. T.; Leclaire, J.; Vial, L.; West, K. R.; Wietor, J.-L.; Sanders, J. K. M.; Otto, S. *Chem. Rev.* **2006**, *106*, 3652–3711. (c) Jin, Y.; Yu, C.; Denman, R. J.; Zhang, W. *Chem. Soc. Rev.* **2013**, *42*, 6634–6654.

(5) (a) Lippert, A. R.; Keleshian, V. L.; Bode, J. W. *Org. Biomol. Chem.* **2009**, *7*, 1529–1532. (b) Lippert, A. R.; Naganawa, A.; Keleshian, V. L.; Bode, J. W. *J. Am. Chem. Soc.* **2010**, *132*, 15790–15799. (c) He, M.; Bode, J. W. *Proc. Natl. Acad. Sci. U. S. A.* **2011**, *108*, 14752–14756. (d) Larson, K. K.; He, M.; Teichert, J. F.; Naganawa, A.; Bode, J. W. *Chem. Sci.* **2012**, *3*, 1825–1828. (e) Teichert, J. F.; Mazunin, D.; Bode, J. W. *J. Am. Chem. Soc.* **2013**, *135*, 11314–11321. (f) He, M.; Bode, J. W. *Org. Biomol. Chem.* **2013**, *11*, 1306–1317.

(6) Saunders, M. *Tetrahedron Lett.* **1963**, *4*, 1699–1702.

(7) Poupko, R.; Zimmermann, H.; Muller, K.; Luz, Z. *J. Am. Chem. Soc.* **1996**, *118*, 7995–8005.

(8) Rebsamen, K.; Roettele, H.; Schroeder, G. *Chem. Ber.* **1993**, *126*, 1429–33.

(9) (a) Ferrer, S.; Echavarren, A. M. *Angew. Chem., Int. Ed.* **2016**, *55*, 11178–11182. (b) McGonigal, P. R.; de León, C.; Wang, Y.; Homs, A.; Solorio-Alvarado, C. R.; Echavarren, A. M. *Angew. Chem., Int. Ed.* **2012**, *51*, 13093–13096.

(10) Yahiaoui, O.; Pašteka, L. F.; Judeel, B.; Fallon, T. *Angew. Chem., Int. Ed.* **2018**, *57*, 2570–2574.

(11) (a) Achard, M.; Mosrin, M.; Tenaglia, A.; Buono, G. *J. Org. Chem.* **2006**, *71*, 2907–2910. (b) D'yakonov, V. A.; Kadikova, G. N.; Dzhemileva, L. U.; Gazizullina, G. F.; Ramazanov, I. R.; Dzhemilev, U. M. *J. Org. Chem.* **2017**, *82*, 471–480.

(12) (a) Jones, M.; Scott, L. T. *J. Am. Chem. Soc.* **1967**, *89*, 150–151. (b) Jones, M.; Reich, S. D.; Scott, L. T. *J. Am. Chem. Soc.* **1970**, *92*, 3118–3126.

(13) de Meijere, A.; Lee, C.-H.; Bengtson, B.; Pohl, E.; Kozhus, S. I.; Schreiner, P. R.; Boese, R.; Haumann, T. *Chem. - Eur. J.* **2003**, *9*, 5481–5488.

(14) In principle these cycloadditions could proceed in any of eight distinct modes, leading to eight regioisomers. In practice the trimethylsilyl group is primarily directed to the bridging alkene. See Supporting Information for full details.

(15) Disubstituted bullvalenes exist as ensembles of either 15 isomers (R_1, R_1) or 30 isomers (R_1, R_2), respectively. Trisubstituted systems will exist as ensembles of 42 (R_1, R_1, R_1), 120 (R_1, R_1, R_2), or 240 isomers (R_1, R_2, R_3), respectively.

(16) This feature was previously described by Bode, ref 5f.

(17) https://kintekcorp.com/, accessed Nov 19, 2019.

(18) (a) Becke, A. D. *J. Chem. Phys.* **1993**, *98*, 5648. (b) Lee, C.; Yang, W.; Parr, R. G. *Phys. Rev. B: Condens. Matter Mater. Phys.* **1988**, *37*, 785. (c) Rappoport, D.; Furche, F. *J. Chem. Phys.* **2010**, *133*, 134105. (d) Barone, V.; Cossi, M. *J. Phys. Chem. A* **1998**, *102*, 1995. (e) Cossi, M.; Rega, N.; Scalmani, G.; Barone, V. *J. Comput. Chem.* **2003**, *24*, 669. (f) Neese, F. *WIREs Comput. Mol. Sci.* **2012**, *2*, 73.

(19) (a) http://hinsberg.net/kinetiscope/, accessed Nov 19, 2019. (b) https://github.com/sbednarz/chemical-kinetics-simulator, accessed Nov 19, 2019.

DOI: 10.1021/acs.orglett.9b03737
Org. Lett. XXXX, XXX, XXX–XXX